Complete phase locking in modulated relaxation oscillators described by a nonsmooth circle map: Positive fractal dimension of the complementary set of phase-locked regions

Kouichi Yagisawa and Takeshi Kambara*
Department of Applied Physics and Chemistry, The University of Electro-Communications, Chofu, Tokyo 182, Japan

Nobuko Fuchikami
Department of Physics, Faculty of Science, Tokyo Metropolitan University, Minami-Ohsawa, Hachioji, Tokyo 192-03, Japan

Masayoshi Naito
Advanced Research Laboratory, Hitachi, Ltd., Hatoyama, Saitama 350-03, Japan
(Received 5 October 1995; revised manuscript received 15 March 1996)

As a model for modulated relaxation oscillators, an integrate-and-fire model in which the sawtooth motion of a state variable is modulated by another sawtooth oscillation is investigated. The dynamics of the system is described by a mapping function that maps successive firing times. The map is a piecewise-linear circle map having two continuous nondifferentiable points or one discontinuous point, which is equivalent to the Poincaré map investigated by Christiansen, Alstrøm, and Levinsen [Phys. Rev. A **42**, 1891 (1990)]. It is proved analytically that a different type of dynamics appears in a nonchaotic region of parameter space in the present system, that is, complete phase locking (CPL) with positive fractal dimension of quasiperiodic set occurs in an entire region where the mapping function describing the system dynamics is monotonic and continuous. It is also shown that the probability of occurrence of periodic orbits with period longer than N is evaluated by a power of N, that is, by $N^{2(1-1/d)}$, where d is the dimension of quasiperiodic set that is positive and less than 1. If the modulation is weak, the dimension d takes a value near 1 and the orbits with very long period appear frequently. When the modulation is enforced, a discontinuity appears in the mapping function. It has been known that a monotonic and discontinuous piecewise linear map results in CPL with zero dimension of quasiperiodicity [B. Chritiansen, P. Alstrøm, and M. T. Levinsen, Phys. Rev. A **42**, 1891 (1990)]. It is identified in the present paper that the transition induced by the occurrence of discontinuity is the one within CPL such that the dimension of quasiperiodicity changes abruptly from a positive number to zero. This is the transition in which the periodic orbits with long period disappear. [S1063-651X(96)00909-9]

PACS number(s): 05.45.+b, 87.10.+e, 02.30.−f, 64.70.Md

I. INTRODUCTION

Modulated relaxation oscillators and their integrate-and-fire models have attracted much attention as they have important applications in many different fields such as biology [1–5], electronics [6–8], and solid state physics [9]. The dynamics of the modulated oscillators can be described by a circle map. Recently, much attention has been paid to the circle maps derived from the modulated integrate-and-fire models. It has been found that the maps have many interesting characteristics that ordinary circle maps do not have. Most of these characteristics are attributable to the appearance of discontinuity in the map. As the modulation is enforced, a discontinuity appears in the map, which results in complete phase locking (CPL) in a finite region of the phase space, in which the quasiperiodicity has zero measure [7,10–14]. Thus a nonchaotic transition from quasiperiodicity to CPL occurs with the appearance of the gap. The dimension of quasiperiodicity is zero [10,13]. This is in contrast to the cases of usual circle maps in which CPL occurs only on the critical line. Crossing the critical line, the phase-locked regions begin to overlap and chaos develops. Thus quasiperiodicity changes into chaos across the line. In maps having both discontinuity and noninvertibility, a different type of intermittency (type V) has been found [15–19]. It has also been found that the interaction between discontinuity and noninvertibility induces complex dynamical behavior [8,20–22].

In the present paper we prove analytically that a different type of complete phase locking occurs in a dynamical system described by a circle map derived from modulated integrate-and-fire models. We show, for monotonic continuous piecewise-linear circle maps having two nondifferentiable points, that CPL with a positive dimension of the quasiperiodic set occurs in an entire region of the phase space. The map was derived as a mapping function that maps successive firing times in an integrate-and-fire system that has a finite resetting time and in which the upper or lower threshold is triangularly modulated.

Christiansen, Alstrøm, and Levinsen [10] made a detailed analysis on a piecewise-linear map, in order to analyze systematically the routes to chaos and CPL occurring in the maps derived from modulated integrate-and-fire models. Their map is the Poincaré map derived from a model where the resetting time is abrupt and both the upper and lower thresholds are triangularly modulated and the map in the present paper has substantially the same structure as theirs. They derived several scaling laws for the cases where the map becomes nonmonotonic and/or discontinuous. For a

*Author to whom correspondence should be addressed.

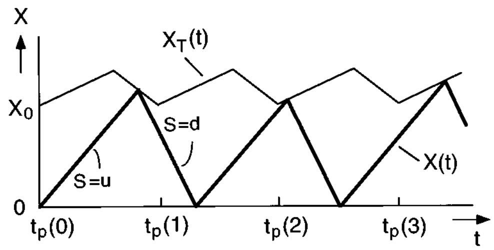

FIG. 1. Schematic of the dynamics of the system.

monotonic and continuous map, they assumed that both periodic (phase locked) and quasiperiodic states were possible based on the values of the Lyapunov exponent the system might take, but did not clarify which dynamics, periodicity or quasiperiodicity, prevailed in that case.

Whereas quasiperiodicity has a positive measure in monotonic and continuous circle maps when the maps are sufficiently smooth [14], the present result shows that the measure of quasiperiodicity can be zero (CPL) for monotonic and continuous, but nonsmooth, maps. The fractal dimension of the quasiperiodic set is positive and less than one in the present map, which is piecewise linear and has two nondifferenciable points. Since the dimension of quasiperiodicity is zero in the case of CPL associated with the discontinuity of the map [10,13], the transition induced by the appearance of the discontinuity is the transition within CPL with which the dimension of quasiperiodicity changes abruptly, as opposed to the transition from the coexistence of quasiperiodicity and phase locking to CPL considered by Christiansen, Alstrøm, and Levinsen [10].

We also show for the present map that, when the map is monotonic and continuous, the measure of the set of parameter values that give the periodic orbits having the period longer than N is evaluated by $N^{2(1-1/d)}$, where d is the dimension of the quasiperiodic set. When the modulation is weak, d takes a value near one. Then the orbits with very long period appear frequently. Because an extraordinarily long period often appears, we cannot distinguish between such periodic orbits and quasiperiodic ones by numerical analysis in which mapping cannot be iterated infinite times. In order to obtain a clear result, an analytical approach is indispensable.

It is proved also in the present paper that when the map is monotonic and discontinuous, the probability of occurrence of orbits with period longer than N decreases exponentially with N, as denoted by Christiansen, Alstrøm, and Levinsen [10]. Thus, from another point of view, the transition induced by the discontinuity in the map is such that the dependence of the probability of a long period on N changes from a power law to an exponential law and the orbits with long period disappear.

II. MODEL

We consider the model in which the ''sawtooth'' motion of a state variable X is modulated by a threshold X_T in a sawtooth way, as shown in Fig. 1. The linear motion of the state variable corresponds to the linear charging and discharging of a capacitance as in the model of Glass and Mackey [1,23]. It also corresponds to one of the simplest version of the model for the self-sustained oscillation of the membrane potential of lipid bilayers [5,24], which is induced by the repetitive gel–liquid-crystal phase transitions of the membrane associated with the adsorption and desorption of protons on the membrane surface, in which the higher-order fluctuation of ion concentration is neglected and there is no external stimulating current.

The present model is similar to that of Christiansen, Alstrøm, and Levinsen [10] in which the resetting is abrupt and both the upper and lower thresholds are modulated triangularly, but the present model has finite resetting time and only the upper threshold is modulated and the lower threshold is set at zero as shown in Fig. 1. The present model is thus a triangular-modulation version of the model considered by Glass and Bélair [3,25] in which the modulation is sinusoidal.

The time evolution of the state variable, or activity, X follows the equation

$$\frac{dX}{dt}=\begin{cases}\alpha_u & \text{for } S(t)=u\\ \alpha_d & \text{for } S(t)=d,\end{cases} \tag{2.1}$$

where α_u (α_d) is the changing rate of X during the ''up'' (''down'') phase in which X is increasing (decreasing). S denotes the state of the system and $S=u$ ($S=d$) means that the system is in the up (down) phase. The state index $S(t)$ is given by

$$S(t)=\begin{cases}u & \text{for } X\leqslant 0\\ d & \text{for } X\geqslant X_T\\ S(t-\Delta t) & \text{for } 0<X<X_T,\end{cases} \tag{2.2}$$

where X_T is the upper threshold. Equation (2.1) shows that the change rate of X is determined by the state S and Eq. (2.2) shows that the phase state is determined by the value of X with hysteresis. The system described by Eqs. (2.1) and (2.2) generates self-sustained oscillations of X and S when $\alpha_u>0$ and $\alpha_d<0$.

We apply a triangular modulation to the upper threshold X_T as

$$X_T(t)=X_0+hY(t), \tag{2.3}$$

where X_0 (>0) is the base line of the upper threshold, h (>0) is a parameter that represents the degree of modulation, and $Y(t)$ varies linearly back and forth in the range from 0 to Y_T (>0) as

$$Y(t)=\begin{cases}\xi_u[t-t_p(n)] \\ \quad \text{for } t_p(n)\leqslant t\leqslant t_p(n)+Y_T/\xi_u\\ \xi_d[t-t_p(n+1)] \\ \quad \text{for } t_p(n)+Y_T/\xi_u\leqslant t\leqslant t_p(n+1).\end{cases} \tag{2.4}$$

Here X_T increases with the rate ξ_u ($\xi_u>0$) and decreases with the rate ξ_d ($\xi_d<0$), $t_p(n)=nY_T(1/\xi_u-1/\xi_d)+\phi$, n is an integer, and ϕ is the phase of the modulating oscillation of $Y(t)$.

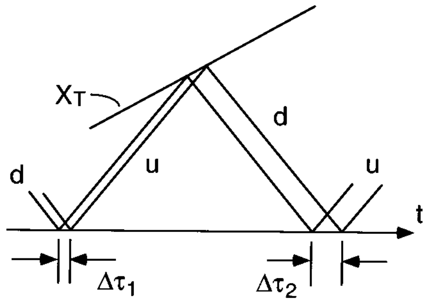

FIG. 2. Orbits separated by $\Delta\tau_1$ in time will, after a $u\rightarrow d$ transition, be separated by $\Delta\tau_2$.

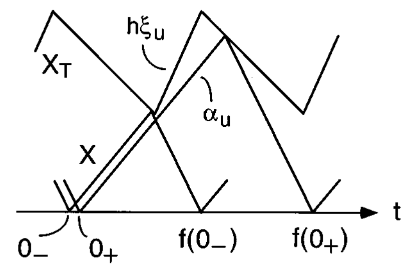

FIG. 3. The mapping function becomes discontinuous when $\alpha_u \leqslant h\xi_u$ because some part of the $u\rightarrow d$ threshold X_T becomes ''invisible.''

III. MAP FOR THE DESCRIPTION OF THE DYNAMICS

A. Derivation of the map

The dynamics of the state variable X described by Eqs. (2.1) and (2.2) under the threshold modulation given by Eqs. (2.3) and (2.4) is completely described by a mapping function that maps successive times at which X reaches the lower threshold, that is, the times at which the transitions from down phase (d) to up phase (u) occur. We derive here the mapping function f for the iterative transition times. Rescaling the time properly, we can assume that the period of threshold modulation is 1 without losing generality. Then, f becomes a circle map of period 1, that is, $f(t+1)=f(t)+1$.

Since the variations of both X and X_T are linear, the map f is piecewise linear (Fig. 4). The slope of f is obtained by calculating a quantity $\Delta\tau_2/\Delta\tau_1$, where $\Delta\tau_1$ is a difference between the transition times at which two nearby orbits undergo the transition from d to u successively and $\Delta\tau_2$ is the time difference for the orbits when they undergo the $d\rightarrow u$ transition the next time as seen in Fig. 2. The value of the slope is changed depending on whether the transition from u to d at which X reaches the upper threshold X_T occurs during the period where X_T is increasing or the transition occurs during the period where X_T is decreasing. If the $u\rightarrow d$ transition occurs when X_T increases with the rate $h\xi_u$, the slope of f is given by

$$D=(1-\alpha_d^{-1}h\xi_u)/(1-\alpha_u^{-1}h\xi_u), \tag{3.1}$$

and if the transition occurs when X_T is decreasing with the rate $h\xi_d$, the slope is given by

$$E=(1-\alpha_d^{-1}h\xi_d)/(1-\alpha_u^{-1}h\xi_d). \tag{3.2}$$

When $\alpha_u > h\xi_u$, the map f is continuous and has two slopes D and E. On the other hand, when $\alpha_u \leqslant h\xi_u$, the map f becomes discontinuous and has only the slope of E. This comes from the fact that the $u\rightarrow d$ transition does not occur when X_T increases, since the increase rate $h\xi_u$ of X_T is larger than that α_u of X and X does not reach X_T. The discontinuity appears at the point where $u\rightarrow d$ transition occurs at a minimum point of X_T as shown in Fig. 3.

We assume that X_T reaches a minimum point at $t=\alpha_u^{-1}X_0$. This can be done by adjusting the phase ϕ of the modulation. Then $t=n$ (integer) becomes the point at which the map f changes the slope (for $\alpha_u > h\xi_u$) or has a discontinuity (for $\alpha_u \leqslant h\xi_u$) as shown in Fig. 4. Finally, we obtain the map f as

$$f(t)=\begin{cases} Dt+B & \text{for } 0\leqslant t\leqslant A \\ Et+B-E+1 & \text{for } A\leqslant t\leqslant 1 \end{cases} \tag{3.3}$$

in the case of $\alpha_u > h\xi_u$ and

$$f(t)=Et+B-E+1 \quad \text{for } 0<t\leqslant 1 \tag{3.4}$$

in the case of $\alpha_u \leqslant h\xi_u$, where

$$A=(1-E)/(D-E) \tag{3.5}$$

and

$$B=(\alpha_u^{-1}-\alpha_d^{-1})X_0. \tag{3.6}$$

In the extended domain $-\infty<t<\infty$, $f(t)$ is defined such that $f(t+n)=f(t)+n$ for any integer n. The map f represented by Eq. (3.4) has a vertical gap of the size $1-E$ at $t=n$.

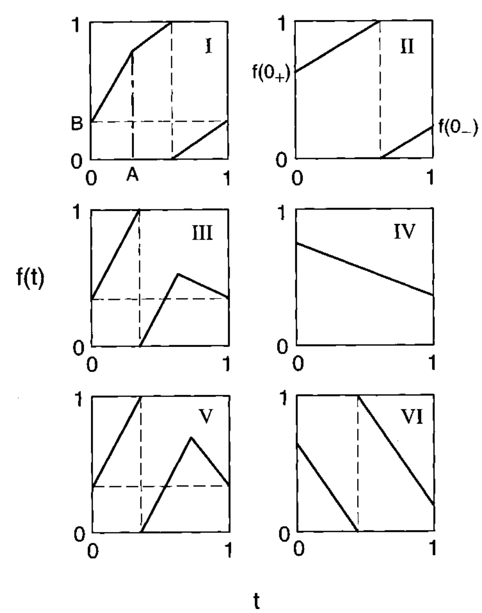

FIG. 4. Graphs of mapping function f (mod1) in different regions of parameter space. The regions correspond to those in Table I.

TABLE I. Different regions in parameter space and the type of solutions. d is the fractal dimension of quasiperiodic set.

Region	Feature of f	Motion
I: $D>1$, $E>0$	monotonic and continuous	CPL, $d>0$
II: $D<0$, $E>0$	monotonic and discontinuous	CPL, $d=0$
III: $D>1$, $-1<E<0$	nonmonotonic and continuous	periodic or chaotic
IV: $D<0$, $-1<E<0$	nonmonotonic and discontinuous	periodic with period 1
V: $D>1$, $E<-1$	nonmonotonic and continuous	chaotic
VI: $D<0$, $E<-1$	nonmonotonic and discontinuous	chaotic

B. Classification of regions in parameter space

When the mapping function f is monotonic, the asymptotic orbit of the state variable X is periodic and/or quasiperiodic, and when f is nonmonotonic, the orbit may become chaotic depending on the values of system parameters. Although the map f in the present system has three parameters D, E, and B, the monotonicity and the continuity of f is determined solely by D and E. The result is summarized in Table I. The map f is monotonic if and only if $E \geqslant 0$. The necessary and sufficient condition for the continuity of f is $D>0$. The condition $D<0$ can be used to classify f as discontinuous, though D does not appear in f when it is discontinuous, since the parameter D defined by Eq. (3.1) is negative when $\alpha_u < h\xi_u$. The orbit of X becomes chaotic when $E<-1$, because $0 \leqslant D < 1$ does not hold as seen from Eq. (3.1) and the absolute value of the slope of f is larger than 1 everywhere when $E<-1$. From these considerations, parameter space is classified into six regions shown in Table I. Typical graphs of f (mod1) in different regions are shown in Fig. 4. The map here is essentially equivalent to the one discussed by Christiansen, Alstrøm, and Levinsen [10].

We are mainly interested in regions I and II in this paper, as mentioned in Sec. I. In region I the map is monotonic, continuous, and piecewise linear and has two nondifferentiable points at $t=0$ and A. In region II the map is monotonic and piecewise linear and has a discontinuity at $t=0$. When a circle map is monotonic and discontinuous like the one in the region II, CPL occurs [10–14,7] and the dimension d of the complementary set of phase-locked regions is zero [13,10]. We will prove in Sec. IV that CPL occurs also in region I and that d is positive. Therefore, the transition from region I to region II associated with the appearance of discontinuity is the transition *within* the CPL region such that the dimension of quasiperiodicity changes abruptly at the transition point, although Christiansen, Alstrøm, and Levinsen [10] suggested that the transition was the one from the coexistence of periodicity and quasiperiodicity to CPL. In region III the orbit of X becomes periodic or chaotic depending on the parameter values and it is periodic with period 1 in region IV because the graph of f intersects with diagonal line and the absolute value of the slope of f is less than 1 at the intersection point.

Figure 5 shows the bifurcation diagram of the present system when the modulation parameter h in Eq. (2.3) is varied. When the modulation is weak, the system is in the newly found region I. With increasing h, the system bifurcates into region II or III depending on whether $h_D<h_E$ or $h_D>h_E$, where $h=h_D$ $(=\alpha_u/\xi_u)$ is the zero point of D^{-1} as seen in Eq. (3.1) and $h=h_E$ $(=\alpha_d/\xi_d)$ is the zero point of E as seen in Eq. (3.2).

IV. DYNAMIC PROPERTIES OF THE SYSTEM WITH A MONOTONIC MAP

In this section we summarize the results obtained in the present study in order to clarify the nature of the nonchaotic transition between regions I and II. We describe only the outlines of proofs of the results obtained. Detailed proofs are given in Ref. [26].

A. Region I

1. Measure of the quasiperiodic set

Here we show that the measure of the quasiperiodic set, i.e., the complementary set of phase-locked regions, is zero in region I where the map f is monotonic and continuous, resulting in complete phase locking. The parameters determining the map f are D, E, and B. We vary B and set D and E at constants satisfying the relations $D>1>E>0$, which are the condition that the system is in region I. Variation of B corresponds to that of the base line X_0 of the upper threshold. As shown in Appendix A, we can restrict the range of B in $0<B\leqslant 1$.

The quasiperiodic set is the set where all the regions of B giving phase locking are removed from the entire region (0,1] of B. Phase locking occurs when the rotation number

$$R=\lim_{n\to\infty}[f^n(t_0)-t_0]/n \tag{4.1}$$

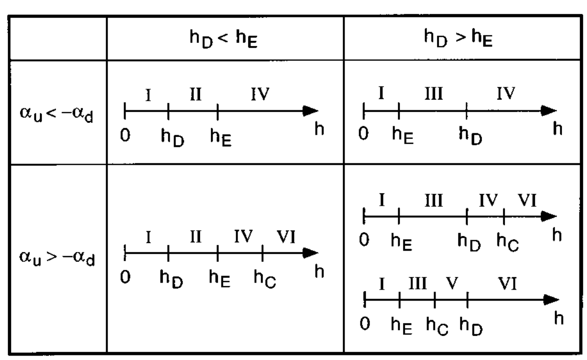

FIG. 5. Bifurcation diagram of the system when the modulation parameter h is varied. $h_D=\alpha_u/\xi_u$ is the zero point of D^{-1}, $h_E=\alpha_d/\xi_d$ is the zero point of E, and $h_C=2\alpha_u\alpha_d/(\alpha_u+\alpha_d)\xi_d$ is the value of h at which $E=-1$.

becomes a rational number. Because the mapping function f is a monotonic function of B as seen in Eq. (3.3), the rotation number is also a monotonic function of B, that is, if $B_1 \leqslant B_2$, then $R(B_1) \leqslant R(B_2)$.

We define the "Q/P-entrainment region" $\mathcal{B}(Q/P)$ as the region of B in which the rotation number R takes an irreducible fraction Q/P $(P>0)$. As shown in Appendix A, it is enough to consider for $0<Q\leqslant P$. Because $R(B)$ is monotonic with B, the Q/P-entrainment region is a closed interval for each value of Q/P. We denote the region as

$$\mathcal{B}(Q/P)=[B_L(Q/P),B_U(Q/P)]. \tag{4.2}$$

Here $B_L(Q/P)$ is the lower boundary and $B_U(Q/P)$ is the upper boundary of the region, that is, $R<Q/P$ for $B<B_L(Q/P)$, $R=Q/P$ for $B_L(Q/P)\leqslant B\leqslant B_U(Q/P)$, and $R>Q/P$ for $B>B_U(Q/P)$. Explicit expressions of these boundaries are derived in Appendixes A and B [Eqs. (A6) and (B1)].

We obtain the quasiperiodic set Δ by removing all $\mathcal{B}(Q/P)$ from the region (0,1]. It is given by

$$\Delta=\lim_{N\to\infty}\Delta_N, \tag{4.3}$$

where Δ_N is a set such that all the entrainment regions having periods equal to or less than N are removed from the region (0,1],

$$\Delta_N=(0,1]-\bigcup_{\substack{P\leqslant N\\ 0<Q\leqslant P}}\mathcal{B}(Q/P). \tag{4.4}$$

As shown in Appendix C, we can prove that the following inequality holds for the Lebesgue measure $\mu(\Delta_N)$ of the set Δ_N:

$$\mu(\Delta_N)\leqslant C_0 N^{-\rho}, \tag{4.5}$$

where C_0 and ρ are positive numbers that depend on D and E but do not depend on N. From the relations (4.3) and (4.5), we obtain

$$\mu(\Delta)=0, \tag{4.6}$$

that is, the measure of quasiperiodic set is zero and CPL occurs in the region I of the parameter space.

2. Dimension of the quasiperiodic set

Here we discuss the fractal dimension of quasiperiodic set Δ. We use the capacity dimension for the fractal dimension. Then we obtain the inequalities for the dimension d of the set Δ,

$$(1+\tfrac{1}{2}\rho)^{-1}\geqslant d\geqslant \max\left(\frac{1}{2},\frac{1}{1+(D/E)^2\{1-(E/D)^{1/4}\}}\right), \tag{4.7}$$

where ρ is the positive number appeared in the inequality (4.5). The derivation of (4.7) is briefly explained in Appendix D. The inequalities (4.7) show that, in the region I, d is positive $(\geqslant\frac{1}{2})$ and less than 1.

The left-hand inequality in (4.7) is derived from the relation between the dimension d and the measure $\mu(\Delta_N)$, which is proved in Appendix D,

$$2\left(1-\frac{1}{d}\right)\leqslant \lim_{k\to\infty}\inf_{k\leqslant N}\frac{\ln\mu(\Delta_N)}{\ln N}. \tag{4.8}$$

This relation provides information on the probability of the occurrence of an orbit having a long period. Because of CPL, the measure of the set Δ_N is equal to that of the set composed of the values of B that generate periodic orbits having periods longer than N. Therefore, inequalities (4.5) and (4.8) indicate that the probability of the occurrence of orbits with periods longer than N is evaluated by a power of N, that is, by $N^{2(1-1/d)}$.

B. Region II

In this subsection we describe the behavior of the system in region II where the map f is monotonic and discontinuous. The parameters determining the map f are E and B. We vary B keeping E constant. The results obtained here coincide with those obtained by Christiansen, Alstrøm, and Levinsen [10], that is, the quasiperiodic set Δ has zero measure and the fractal dimension of the set is zero.

The set Δ_N defined in Eq. (4.4) is rewritten as

$$\Delta_N=\bigcup_i J_i, \tag{4.9}$$

where

$$J_i=(B_U(q_i/p_i),B_L(q_{i+1}/p_{i+1})) \tag{4.10}$$

and irreducible fractions q_i/p_i and q_{i+1}/p_{i+1} form a neighboring pair in a Farey series associated with integer N. We proved (see Appendix E) the inequality for the measure of J_i,

$$(1-E)^2E^{p_i+p_{i+1}-1}<\mu(J_i)\leqslant E^N. \tag{4.11}$$

Since there is at least one pair of p_i and p_{i+1} that satisfies $p_i+p_{i+1}=N+1$ and since the number of the elements in a Farey series associated with N is less than N^2 for $N\geqslant 2$, the measure of Δ_N satisfies the inequality

$$(1-E)^2E^N<\mu(\Delta_N)\leqslant N^2E^N. \tag{4.12}$$

It is concluded, from (4.3) and (4.12), that the measure of the set Δ is zero because $E<1$, as seen from Eq. (3.2).

As seen from the above argument, the set Δ_N can be covered by at most N^2 open intervals with length E^N. Then the dimension d of Δ is obtained as

$$d=\lim_{N\to\infty}\frac{\ln N^2}{\ln E^N}=0. \tag{4.13}$$

The inequality (4.12) shows that the probability of the occurrence of a long period decreases with N exponentially.

It is noted in the case of $E=0$ and $D>0$ that the system obeys the results for region II in which the map f is discontinuous, although f is actually continuous. Interchanging the abscissa and the ordinate in the graph of f and interpreting

D^{-1} as E, we obtain a new map that has a single slope E and discontinuity (Fig. 4, region II). Then, the results obtained for region II apply to that map because the interchange of coordinates does not affect periodicity or quasiperiodicity when a map is monotonic.

V. DISCUSSION

In region I studied in detail in the present paper, the probability of the occurrence of orbits with very long period larger than N is evaluated by $N^{2(1-1/d)}$. When the modulation of the threshold is small, this probability is high. For a small value of the modulation parameter h, E/D takes the value near 1 as seen from Eqs. (3.1) and (3.2). Then, the value of the fractal dimension d becomes near 1 as seen from the inequality (4.7) and $N^{2(1-1/d)}$ is considerably large even for very large values of N. Orbits with very long period have been confirmed. We can calculate the value of the rotation number R when the values of the parameters D, E, and B are given, by using Eqs. (A6) and (B1). The calculation showed that orbits with a long period appear frequently as the values of D and E approach 1 and that a very long period with astronomical order appears sometimes. For example, for $D=1.3$, $E=0.9$, and $B=0.3$, the period of the attractor was found to be about $P\approx 2.29\times 10^{72}$, where the rotation number was $R=Q/P\approx 0.336$ with $\mu(\mathcal{B}(Q/P))$ being about 2.20×10^{-148}. The Lyapunov exponent, which is given by $\lambda=P^{-1}\ln(D^{[Pr]}E^{P-[Pr]})$, where r is defined in Eq. (B9), was about -1.33×10^{-73}. The orbits with such a long period cannot be identified in fact as periodic, but would be identified as quasiperiodic when we use only the numerical analysis of dynamical systems in which a mapping function cannot be iterated infinite times. For the systems where Poincaré map is nonsmooth, the probability of the occurrence of periodic orbits with long period may be high. Therefore, we should be careful in identifying quasiperiodicity.

We consider how high the probability of the occurrence of orbits with a long period is in region I. We can prove that the expectation value of the period P becomes infinite as follows. Because of the complete phase locking, the rotation number R is rational for all values of B except the set with Lebesgue measure zero, and thus the period P of an orbit, which is the denominator of R, is a Lebesgue measurable function of B. Therefore, we can make Lebesgue integration of a quantity P^{η}, where η is a positive number, in the range $0<B\leq 1$ and consider the value of the integral as the expectation value of P^{η}. From the relation (4.8), it is derived that the expectation value $A_P(\eta)$ of P^{η} becomes infinite for $\eta>2(d^{-1}-1)$. Let η_0 be a positive number that satisfies the relation $\eta>\eta_0>2(d^{-1}-1)$. From the inequality (4.8), the relation $\mu(\Delta_N)\geq N^{-\eta_0}$ holds for large N. Then we obtain the relationship $A_P(\eta)\geq N^{\eta}N^{-\eta_0}$ because the period P exceeds N on the set Δ_N. $A_P(\eta)$ becomes infinite in the limit $N\to\infty$. When h is small and E/D takes a value near 1, which is the condition of the occurrence of a long period, the expectation value $A_P(1)$ of period P becomes infinite because $1>2(d^{-1}-1)$ when $(D/E)^2[1-(E/D)^{1/4}]<\frac{1}{2}$.

In region II of the parameter space, the probability for the occurrence of the orbits with a period longer than N decreases with N exponentially, as seen from the relationship (4.12). Therefore, physically, the transition induced by the occurrence of a discontinuity in the map is the one in which the periodic orbits with long period disappear.

Although quasiperiodicity has zero measure in region I of the parameter space, the appearance of quasiperiodicity is not excluded for special values of the parameters with Lebesgue measure zero. Here we give two cases where quasiperiodicity appears. One of the cases is as follows. When the parameter values are such that a relation $f^n(0)=A+m$ or $f^n(A)=m$ holds for some integers n and m, the rotation number R becomes $R=(m+r)/n$ or $(m-r)/n$, respectively. Then the orbit becomes quasiperiodic when r is irrational. In the other case, the rotation number R becomes irrational as a solution to a quadratic equation. We can show that when D, E, and B satisfy specific relations, for example,

$$D=x\left\{1+\frac{x}{m_1m_2(1+x)}\right\}, \tag{5.1}$$

$$B=m_2\,\frac{m_1(1+x)-x}{x^2+m_1m_2(1+x)^2}, \tag{5.2}$$

$$E=1/D, \tag{5.3}$$

where x is a positive real number and m_1 and m_2 are integers, then the rotation number R becomes

$$R=\frac{1}{2}\left(1+m_2\left\{1-\sqrt{1+\frac{1}{m_1m_2}}\right\}\right). \tag{5.4}$$

An example of irrational R is as follows. We can choose two positive integers p and q that satisfy a relation $q^2=np^2+1$ where n is a nonsquare number and set $m_1=q^2$ and $m_2=-1$. Then R becomes $R=(p/2q)\sqrt{n}$.

It might be difficult to observe the periodic motion with very long period, not only numerically but also in experiments, because the contamination from noise is inevitable in actual systems. When a periodic orbit with very long period is disturbed by noise, the orbit would not be distinguishable from quasiperiodic one with noise. However, in that case, such apparently quasiperiodic motion is the result of superimposition of noise and the inherent dynamics itself is periodic. Since identifying directly the extraordinarily long period is difficult both by numerical calculation and by experiment, an analytical approach adopted in the present paper is indispensable in order to know the substance of the dynamics. Now that we know the dynamics of the system described by the map considered here, it is highly possible that the inherent dynamics of a system is a periodic one having a long period when a map obtained experimentally is such that the map in the present paper, or its equivalent, is blurred due to noise.

Recently, we presented a model of lipid-bilayer membrane in order to clarify the mechanism of self-sustained oscillation of the electric potential across the membrane [24,5]. The model in the present paper is considered to describe the dynamics of the lipid-bilayer membrane operating under a special condition. In the previous model [24], the oscillation of the membrane potential is driven by the repetitive gel–liquid-crystal phase transitions of the membrane. The transitions are generated by the repetitive adsorption and desorption of protons on the membrane surface that are induced by periodic or aperiodic reversal of the direction of protonic current. The gel state is stabilized by the proton adsorption, while the liquid-crystal state is stabilized by the proton desorption. This previous model was simplified to a one-variable representation [5]. The simplified model describes the evolution of proton concentration at the membrane surface driven by repetitive phase transitions between the gel and liquid-crystal states of the membrane. The transition from the gel to the liquid-crystal states occurs when the proton concentration decreases below a threshold value and the reverse transition occurs when the proton concentration increases above another threshold value. The threshold value for the forward transition becomes generally different from that for the reverse transition. The model showed complete phase locking as well as periodicity, quasiperiodicity, and chaos under the application of a sinusoidal stimulating electric current, and the routes to chaos were clarified. The simplified model of the lipid bilayer was named ''the model of repetitive phase transition with hysteresis (RPTH model),'' where the phase transition of lipid bilayer membranes has hysteresis.

The present model corresponds to one of the simplest version of RPTH model for which a temperature modulation is applied. With the variation of temperature, the threshold values of the proton concentration at which the lipid bilayer undergoes the gel–liquid-crystal phase transitions vary with time because the amount of protons required to induce the transition depends on the temperature: the gel (liquid-crystal) state is stabilized with decreasing (increasing) temperature [24]. The present model corresponds to the case where the threshold value is modulated only for the transition from the liquid-crystal state to the gel state and the modulation is triangular and where the higher-order fluctuation of ion concentration is negligible and the proton concentration varies linearly with time.

In more realistic cases, the variable X varies exponentially with time and the map f is no longer piecewise linear when damping factors appear on the right-hand sides of the equation of motion (2.1). When both the upper and lower thresholds are modulated, four nondifferentiable points appear in the map f in modulo 1. We cannot apply the mathematical results obtained in the present paper directly to those cases. We tried numerical experiments using maps having nonlinearity that corresponded to the damping. The results showed that the probability of the occurrence of a long period was similar between these maps and the linear one. So similar results are expected for the occurrence of CPL and the fractal dimension of quasiperiodic set in more general cases. However, the result that $d \geq \frac{1}{2}$ holds in region I, which comes from one of the terms on the right-hand side of (4.7), is an exception. This inequality does not hold generally because it depends on the property of the system that the width of the entrainment region $[B_L(Q/P), B_U(Q/P)]$ is proportional to the quantity $|\langle\langle P\rangle\rangle|$ defined in Eq. (C7) and this property does not hold in general when the mapping function is not piecewise linear or when it has more than two nondifferentiable points in modulo 1. Even then, d is still expected to be positive, though there is a possibility that d goes to $0+$ just before the mapping function becomes discontinuous.

In the present paper, we have clarified the dynamical behavior of the systems described by a monotonic continuous piecewise-linear circle map having two nondifferentiable points. An exact analytical study for a wider class of nonsmooth mapping functions has not yet been obtained and remains as a future task.

APPENDIX A: SYMMETRY PROPERTIES OF THE MAP

Here we show that the range of the parameter B can be restricted to $0<B\leq 1$ and that it is enough to consider the irreducible fraction Q/P for $0<Q\leq P$. In region I, the map $f(t)$ is defined by Eqs. (3.3) and (3.5), where $D>1>E>0$. To show the B dependence explicitly, we denote the map f as $f(t;B)$. The parameter B defined by Eq. (3.6) must be positive, but at first we assume B in the extended domain $-\infty<B<\infty$ for convenience.

First, we note that the map $f(t;B)$ satisfies

$$f^P(t;B+n)=f^P(t;B)+nP \tag{A1}$$

for any integer n (we assume P as a positive integer). Therefore,

$$\text{if } B\in\mathcal{B}\left(\frac{Q}{P}\right) \quad \text{then } B+n\in\mathcal{B}\left(\frac{Q}{P}+n\right), \tag{A2}$$

where $\mathcal{B}(Q/P)$ is the Q/P-entrainment region.

The map has another symmetry property. If we rotate the graph $f(t;B)$ vs t by π around the point $(A/2,A/2)$, we obtain the transformation

$$f(t;B)\to f[t;-B-(D-1)A]. \tag{A3}$$

This leads to

$$R(B)=-R[-B-(D-1)A], \tag{A4}$$

namely,

$$\text{if } B\in\mathcal{B}\left(\frac{Q}{P}\right) \quad \text{then } -B-(D-1)A\in\mathcal{B}\left(-\frac{Q}{P}\right). \tag{A5}$$

From Eqs. (A2) and (A5), we find

$$B_L\left(\frac{Q}{P}\right)=1-(D-1)A-B_U\left(\frac{P-Q}{P}\right), \tag{A6}$$

$$B_U\left(\frac{Q}{P}\right)=1-(D-1)A-B_L\left(\frac{P-Q}{P}\right), \tag{A7}$$

where B_L and B_U are the lower and upper boundaries of the region $\mathcal{B}(Q/P)$. Thus we obtain

$$\mu\left[\mathcal{B}\left(\frac{Q}{P}\right)\right]=\mu\left[\mathcal{B}\left(\frac{P-Q}{P}\right)\right], \tag{A8}$$

where $\mu[\mathcal{B}]$ denotes the Lebesgue measure of the set $\mathcal{B}$. Owing to these symmetry properties, it is enough to consider only for $0<B\leq 1$ and $0<Q\leq P$.

APPENDIX B: DERIVATION OF THE UPPER BOUNDARY $B_U(Q/P)$

The upper boundary $B_U(Q/P)$ of the Q/P-entrainment region $\mathcal{B}(Q/P)$ is given by

$$B_U(Q/P)=T(Q/P)/S(Q/P). \tag{B1}$$

Quantities $S(Q/P)$ and $T(Q/P)$ in this equation are given by

$$S(Q/P)=\sum_{i=1}^{P} U(Q/P,i), \tag{B2}$$

$$T(Q/P)=\sum_{i=1}^{P} U(Q/P,i)V(Q/P,i), \tag{B3}$$

where

$$U(Q/P,1)=1, \tag{B4}$$

$$U(Q/P,i+1)=U(Q/P,i)W(Q/P,i) \quad \text{for } 1\leqslant i\leqslant P-1, \tag{B5}$$

with $W(Q/P,i)$ and $V(Q/P,i)$ defined by

$$W(Q/P,i)=\begin{cases} D & \text{when } 0\leqslant k+Qi(\text{mod } P)\leqslant k-1 \\ E & \text{when } k+1\leqslant k+Qi(\text{mod } P)\leqslant P-1, \end{cases} \tag{B6}$$

$$V(Q/P,i)=\begin{cases} 1 & \text{when } 0\leqslant k+Qi(\text{mod } P)\leqslant Q-1 \\ 0 & \text{when } Q\leqslant k+Qi(\text{mod } P)\leqslant P-1. \end{cases} \tag{B7}$$

The integer k is defined by

$$k=[Pr], \tag{B8}$$

where r is given by

$$r=-\ln(E)/\ln(D/E) \tag{B9}$$

and $[x]$ denotes the Gauss symbol, the maximum integer that is not larger than x.

In order to derive Eq. (B1), we first note that B is equal to $B_U(Q/P)$ when it satisfies

$$f^P(0;B)=Q. \tag{B10}$$

This equation is obtained as follows. Since the map $f(t;B)$ is monotonic and piecewise linear, having two points $t=0$ and A at which the slope is discontinuous, the map $f^P(t;B)$ is also monotonic and piecewise linear, having $2P$ points for $0\leqslant t<1$ at which the slope is discontinuous. For $B\in\mathcal{B}(Q/P)$, $f^P(t;B)$ must intersect with the line $g(t)=t+Q$ [(a) in Fig. 6]. Specifically, when B satisfies Eq. (B10), the function becomes tangent to the line $g(t)$ at P points [(b) in Fig. 6]. This means that B satisfying Eq. (B10) is the upper boundary of $\mathcal{B}(Q/P)$ (see [26] for rigorous proof).

Next, let us define P numbers $f^n(0;B_U(Q/P))$ (mod 1) $(n=0,1,..,P-1)$ in increasing order as $0=x_0<x_1<\cdots<x_{P-1}<1\equiv xp$. Then we find that

$$f(x_i;B_U(Q/P))(\text{mod } 1)=x_{i+Q(\text{mod } P)}, \tag{B11}$$

as a result of Eq. (B10). Since $B=f(0;B)$ as seen from Eq. (3.3), $B_U(Q/P)$ is given by

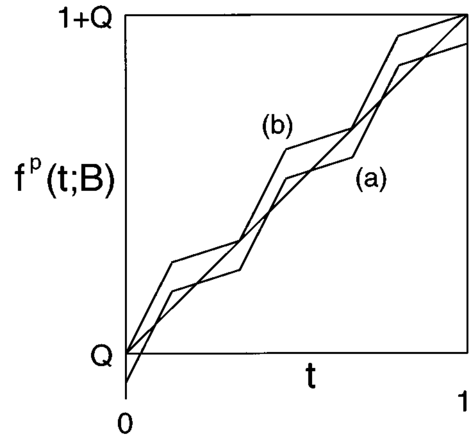

FIG. 6. Graph of the map $f^P(t;B)$ in the case of $P=3$.

$$B_U(Q/P)=f(0;B_U(Q/P))=f(x_0;B_U(Q/P))$$
$$=x_Q=\sum_{i=0}^{Q-1}\mu(I_i), \tag{B12}$$

where we have defined P intervals $I_n\equiv[x_n,x_{n+1})$ $(n=0,1,\ldots,P-1)$.

In the following, we will calculate $\Sigma_{i=0}^{Q-1}\mu(I_i)$. We begin with showing that the point A, at which the slope of the mapping function $f(t;B_U(Q/P))$ is discontinuous, is on the interval I_k where the integer k is given by Eq. (B8). We note, from Eq. (B11), that the interval I_n is mapped on I_m with $m=n+Q$ (mod P):

$$\tilde{f}(I_n)\equiv f(I_n;B_U(Q/P))(\text{mod } 1)=I_{n+Q(\text{mod } P)}. \tag{B13}$$

If an interval I_n is contained in the interval $[0,A)$, on which the slope is D, then I_n is expanded by a factor D by the map $\tilde{f}$, which means

$$\mu(I_{n+Q(\text{mod } P)})=D\mu(I_n) \quad \text{for } 0\leqslant n\leqslant k-1 \tag{B14}$$

when $A\in I_k$. Similarly, an interval I_n on which the slope is E is contracted by the map

$$\mu(I_{n+Q(\text{mod } P)})=E\mu(I_n) \quad \text{for } k+1\leqslant n\leqslant P-1. \tag{B15}$$

For the interval I_k that includes the point A at which the slope changes from D to E, we obtain

$$\mu(I_{k+Q(\text{mod } P)})=F\mu(I_k), \tag{B16}$$

where the factor F is given by

$$F=\{D(A-x_k)+E(x_{k+1}-A)\}/(x_{k+1}-x_k) \tag{B17}$$

satisfying $E\leqslant F<D$.

Starting from I_0, we return to I_0 after P successive mappings of $\tilde{f}$: $I_0\rightarrow I_Q\rightarrow I_{2Q(\text{mod } P)}\rightarrow\cdots\rightarrow I_{PQ(\text{mod } P)}=I_0$. Then, taking account of Eqs. (B14)–(B16), we obtain

$$D^kE^{P-k-1}F\mu(I_0)=\mu(I_0). \tag{B18}$$

Taking logarithms of the above equation, we obtain $k=[Pr]$, which is Eq. (B8).

In the following, we employ the abbreviation $j \equiv k+Q$ (mod P). Then, the condition under which the interval $\tilde{f}^{\,i-1}(I_j)$ coincides with one of the intervals $I_0, I_1, \ldots, I_{Q-1}$ is $0 \leqslant k+Qi$ (mod P) $\leqslant Q-1$. Therefore,

$$\sum_{n=0}^{Q-1} \mu(I_n) = \sum_{i=1}^{P} \mu(\tilde{f}^{\,i-1}(I_j)) V(Q/P,i), \qquad \text{(B19)}$$

where the definition of $V(Q/P,i)$, Eq. (B7), is used. We can prove, by induction, that

$$\mu(\tilde{f}^{\,i-1}(I_j)) = \mu(I_j) U(Q/P,i) \quad (i=1,2,\ldots,P). \qquad \text{(B20)}$$

Substituting Eq. (B20) into Eq. (B19), we obtain

$$\sum_{n=0}^{Q-1} \mu(I_n) = \mu(I_j) \sum_{i=1}^{P} U(Q/P,i) V(Q/P,i). \qquad \text{(B21)}$$

The quantity $\mu(I_j)$ is obtained as follows. Because the set $\{I_j, \tilde{f}(I_j), \ldots, \tilde{f}^{P-1}(I_j)\}$ coincides with $\{I_0, I_1, \ldots, I_{P-1}\}$, we obtain, from Eq. (B20),

$$\mu(I_j) \sum_{i=1}^{P} U(Q/P,i) = \sum_{n=0}^{P-1} \mu(I_n) = 1. \qquad \text{(B22)}$$

From Eqs. (B12), (B21), and (B22), with the definitions of $S(Q/P)$ and $T(Q/P)$ [Eqs. (B2) and (B3)], we see that Eq. (B1) holds.

APPENDIX C: OUTLINE OF PROVING INEQUALITY (4.5)

The measure $\mu(\Delta_N)$ can be obtained by evaluating the measure $\mu[\mathcal{B}(Q/P)]$ of the region $\mathcal{B}(Q/P)$ as seen from Eq. (4.4). The boundaries of the region are given by Eqs. (A6) and (B1).

Our fundamental strategy for proving inequality (4.5) is as follows. We want to know how $\mu(\Delta_N)$ changes with N. The irreducible fractions Q/P appearing in Eq. (4.4) form a Farey series associated with the integer N. The Farey series associated with $N+1$ is formed by adding several ''mediants'' Q'/P' (with $P'=N+1$) between the neighboring irreducible fractions Q_j/P_j and Q_{j+1}/P_{j+1} belonging to the previous series associated with N. Therefore, as N increases, we need to evaluate the measure $\mu(\mathcal{B}(Q'/P'))$ for newly born mediants. For this purpose, we use the following property, the proof of which is given in [26]: when $P_1Q_2 - P_2Q_1 = 1$, i.e., when two irreducible fractions Q_1/P_1 and Q_2/P_2 ($Q_1/P_1 < Q_2/P_2$) are neighboring each other in a Farey series, S and T [Eqs. (B2) and (B3)] for the mediant $(Q_1+Q_2)/(P_1+P_2) \equiv Q/P$ are given by

$$S\left(\frac{Q}{P}\right) = \begin{cases} S(Q_1/P_1) + G_1 S(Q_2/P_2) \\ \quad \text{when } [Pr] = [P_1 r] + [P_2 r] \\ G_2 S(Q_1/P_1) + S(Q_2/P_2) \\ \quad \text{when } [Pr] = [P_1 r] + [P_2 r] + 1, \end{cases} \qquad \text{(C1)}$$

$$T\left(\frac{Q}{P}\right) = \begin{cases} T(Q_1/P_1) + G_1 T(Q_2/P_2) \\ \quad \text{when } [Pr] = [P_1 r] + [P_2 r] \\ G_2 T(Q_1/P_1) + T(Q_2/P_2) \\ \quad \text{when } [Pr] = [P_1 r] + [P_2 r] + 1, \end{cases} \qquad \text{(C2)}$$

where

$$G_1 = D^{[P_1 r]} E^{P_1 - [P_1 r]}, \qquad \text{(C3)}$$

$$G_2 = D^{[P_2 r]+1} E^{P_2 - [P_2 r] - 1}. \qquad \text{(C4)}$$

Many inequalities necessary for our proof are derived from the above property. One of them is given as follows: when $P_0 Q - P Q_0 = 1$ is satisfied for two irreducible fractions Q_0/P_0 and $Q/P (Q_0/P_0 < Q/P)$, the inequality

$$\mu[\mathcal{B}(Q/P)] \geqslant \xi \{ B_L(Q/P) - B_U(Q_0/P_0) \}, \qquad \text{(C5)}$$

holds, where

$$\xi = |\langle\langle P \rangle\rangle| \, \frac{2E}{D} \left\{ 1 - \left(\frac{E}{D}\right)^{1/4} \right\} \frac{S(Q_0/P_0)}{S(Q/P)}, \qquad \text{(C6)}$$

$$\langle\langle P \rangle\rangle = Pr - [Pr + \tfrac{1}{2}]. \qquad \text{(C7)}$$

The proof of this inequality will be published elsewhere [26] because it requires lengthy arguments.

If we could find a suitable number δ (<1) that is independent of N and satisfies an inequality like $\mu(\Delta_{N+1})/\mu(\Delta_N) \leqslant \delta$, the inequality would guarantee $\mu(\Delta_N)$ converging to zero faster than δ^N. But this does not hold. Instead, we can derive a relation as $\mu(\Delta_{4N})/\mu(\Delta_N) \leqslant \rho_0$ (<1) [Eq. (C12)], which yields a slower convergence of $\mu(\Delta_N)$ as $N^{\ln \rho_0 / \ln 4}$. Deriving the inequality directly from the relation (C5) is not easy, however, because the factor $|\langle\langle P \rangle\rangle|$, and so ξ, may become very small for some values of P. Therefore, we adopt the following procedure, instead of estimating $\mu(\Delta_N)$ directly.

For a given small number ε $(0 < \varepsilon < \frac{1}{2})$, we define N_0 as the minimum positive integer that satisfies $|\langle\langle N_0 \rangle\rangle| \geqslant \varepsilon$. For each integer N that is not smaller than N_0, we consider a set $\Delta'_N(\varepsilon)$ $(\supset \Delta_N)$, which is defined as follows, depending on ε. Let us write a Farey series associated with N as

$$\frac{0}{1} = \frac{Q_0}{P_0} < \frac{Q_1}{P_1} < \frac{Q_2}{P_2} < \cdots < \frac{Q_{M-1}}{P_{M-1}} < \frac{Q_M}{P_M} = \frac{1}{1} \quad (1 < P_j \leqslant N \quad \text{for } 0 < j < M). \qquad \text{(C8)}$$

For given ε, we first subtract the interval $\mathcal{B}(Q_M/P_M)$ $[=\mathcal{B}(1/1)]$ together with all intervals $\mathcal{B}(Q_j/P_j)$ such that $|\langle\langle P_j \rangle\rangle| \geqslant \varepsilon$ from the interval (0,1]. Now there are rather narrow intervals left. When there are any (one or more) intervals $\mathcal{B}(Q_{a+1}/P_{a+1}), \mathcal{B}(Q_{a+2}/P_{a+2}), \ldots, \mathcal{B}(Q_{b-1}/P_{b-1})$ between two neighboring intervals $\mathcal{B}(Q_a/P_a)$ and $\mathcal{B}(Q_b/P_b)$ that have been subtracted because of the conditions $|\langle\langle P_a \rangle\rangle| \geqslant \varepsilon$ and $|\langle\langle P_b \rangle\rangle| \geqslant \varepsilon$, we subtract the interval among them that has the minimum denominator P_k,

$$P_k = \min(P_{a+1}, P_{a+2}, \ldots, P_{b-1}). \qquad \text{(C9)}$$

The resultant set thus obtained is defined as $\Delta'_N(\varepsilon)$. The set $\Delta'_N(\varepsilon)$ is therefore a sum of open intervals such as $[B_U(Q_l/P_l), B_L(Q_m/P_m)]$, where $P_l, P_m \leqslant N$ and at least one of $|\langle\langle P_l \rangle\rangle|$ and $|\langle\langle P_m \rangle\rangle|$ is not less than ε. Then we can prove [26], using the relationships (C1) and (C2) and choosing a suitable value for ε that should be neither too large nor too small (actually we may set ε=1/40), that the inequality

$$\sum_{q/p} \mu[\mathcal{B}(q/p)] \geq (1-\rho_0)\{B_L(Q_m/P_m) - B_U(Q_l/P_l)\} \tag{C10}$$

holds, where $(B_U(Q_l/P_l), B_L(Q_m/P_m))$ is any one of open intervals contained in $\Delta_N'(\varepsilon)$ and ρ_0 is a positive number taking a value smaller than 1 that depends on ε but not on N, nor the choice of the interval in $\Delta_N'(\varepsilon)$. The summation on the left-hand side of the inequality (C10) is taken over irreducible fractions q/p such that

$$\frac{Q_l}{P_l} < \frac{q}{p} < \frac{Q_m}{P_m}, \quad N < p \leq 4N. \tag{C11}$$

From the relations (4.4) and (C10), we can easily prove the inequality

$$\mu(\Delta_{4N}) \leq \rho_0 \mu(\Delta_N) \quad \text{for } N \geq N_0. \tag{C12}$$

We obtain the inequality (4.5) from the inequality (C12) by defining $\rho = \ln(1/\rho_0)/\ln 4$ and $C_0 = (4N_0)^\rho$.

APPENDIX D: OUTLINE OF THE DERIVATION OF INEQUALITIES (4.7) AND (4.8)

The expression (4.7) is composed of the three inequalities

$$d \geq 1/(1+C_S^{-1}), \tag{D1}$$

$$d \geq \tfrac{1}{2}, \tag{D2}$$

$$d \leq 1/(1+\rho/2), \tag{D3}$$

where

$$C_S = \left(\frac{E}{D}\right)^2 \Big/ \left\{1 - \left(\frac{E}{D}\right)^{1/4}\right\} \tag{D4}$$

and ρ is the positive number appearing in inequality (4.5). Here we only give an outline of derivation of (D1) and (D3). The proof of (D2) is presented elsewhere [26].

In order to derive (D1), we introduce the following expression for the fractal dimension $d_F(H)$ of a set H, a bounded set of real numbers, which can be derived from the usual definition of the capacity dimension

$$d_F(H) = 1 - \lim_{\varepsilon \to 0+} \sup_{0<\delta\leq\varepsilon} \left\{\frac{\ln \mu(S_F(H,\delta))}{\ln \delta}\right\}, \tag{D5}$$

where $S_F(H,\delta)$ is the sum of the open intervals $(x-\delta, x+\delta)$ for all $x \in H$: $S_F(H,\delta) \equiv \cup_{x\in H}(x-\delta, x+\delta)$. Then, we can evaluate d $[=d_F(\Delta)]$ by evaluating $\mu(S_F(\Delta,\delta))$.

We first present an inequality

$$B_L\left(\frac{Q_2}{P_2}\right) - B_U\left(\frac{Q_1}{P_1}\right) \geq \begin{cases} \left\{B_U\left(\frac{Q_2}{P_2}\right) - B_L\left(\frac{Q_2}{P_2}\right)\right\} C_S & \text{when } P_1 \leq P_2 \\ \left\{B_U\left(\frac{Q_1}{P_1}\right) - B_L\left(\frac{Q_1}{P_1}\right)\right\} C_S & \text{when } P_1 > P_2, \end{cases} \tag{D6}$$

which holds for $Q_1/P_1 < Q_2/P_2$. The proof of this inequality is given in [26].

Next, let $\Delta_F(\delta)$ be the set which is obtained by removing all the entrainment regions of length equal to or larger than 2δ from the interval (0,1]. From the definition of $\Delta_F(\delta)$ and the inequality (D6), $\Delta_F(\delta)$ is expressed as the sum of disconnected intervals $L_1, L_2, \ldots,$ each of which has the length equal to or larger than $2\delta C_S$. Namely,

$$\Delta_F(\delta) = \bigcup_i L_i, \tag{D7}$$

where $L_i \cap L_j = \phi$ for any $i \neq j$ and $\mu(L_i) \geq 2\delta C_S$ for all i. Now, for any interval L of length not smaller than $2\delta C_S$, we can easily show, from the definition of $S_F(L,\delta)$,

$$\mu(S_F[L,(1+\eta)\delta]) \leq \mu(S_F(L,\delta))\left(1 + \frac{\eta}{1+C_S}\right), \tag{D8}$$

where η is any positive number. Applying the above inequality for each L_i in (D7) and noting that $S_F(\Delta,\delta) = S_F[\Delta_F(\delta),\delta]$ and $S_F[\Delta,(1+\eta)\delta] = S_F[\Delta_F(\delta), (1+\eta)\delta]$ hold by definition, we obtain

$$\mu(S_F[\Delta,(1+\eta)\delta]) \leq \mu(S_F(\Delta,\delta))\left(1 + \frac{\eta}{1+C_S}\right). \tag{D9}$$

We substitute $\delta = (1+\eta)^{-m}$ for $m = 1,2,\ldots,n$ into (D9) successively and obtain

$$\mu(S_F(\Delta,1)) \leq \mu(S_F[\Delta,(1+\eta)^{-n}])[1+\eta(1+C_S)^{-1}]^n. \tag{D10}$$

Taking the logarithm of (D10), dividing it by $\ln(1+\eta)^{-n}$, and taking the limit $n \to \infty$, we obtain

$$\lim_{\varepsilon\to 0+} \sup_{0<\delta\leq\varepsilon} \left\{\frac{\ln[\mu(S_F(\Delta,\delta))]}{\ln \delta}\right\} \leq \frac{\ln[1+\eta(1+C_S)^{-1}]}{\ln(1+\eta)}, \tag{D11}$$

where $(1+\eta)^{-n}$ was replaced by δ. Taking the limit $\eta \to 0+$ in the inequality (D11) and using (D5) with $H=\Delta$, we finally obtain the inequality (D1).

The inequality (D3) is derived from inequalities (4.5) and (4.8). We show here the outline of deriving inequality (4.8). For this purpose, we use the expression for the fractal dimension d of Δ,

$$1 - \frac{1}{d} = \lim_{k\to\infty} \inf_{n\geq k} \frac{\ln \mu(\Lambda_S(n))}{\ln n}, \tag{D12}$$

where $\Lambda_S(n)$ is the set that has the minimum measure among such sets that are obtained by removing n entrainment regions from the interval (0,1]. The proof of (D12) is presented elsewhere [26].

From the definition of $\Lambda_S(n)$, we note that

$$\mu(\Delta_N) \geqslant \mu(\Lambda_S(N^2)) \tag{D13}$$

because the number of the entrainment regions $\mathcal{B}(Q/P)$ satisfying $0 < P \leqslant N$ and $0 < Q \leqslant P$ is not larger than N^2. Substitution of $n = N^2$ and (D13) into (D12) leads to the inequality (4.8).

APPENDIX E: OUTLINE OF THE DERIVATION OF INEQUALITY (4.11)

In this appendix we show that a relationship

$$B_L\left(\frac{Q_2}{P_2}\right) - B_U\left(\frac{Q_1}{P_1}\right) = \frac{(1-E)^2 E^{P_1+P_2-1}}{(1-E^{P_1})(1-E^{P_2})} \tag{E1}$$

holds in region II for any two irreducible fractions Q_1/P_1 and Q_2/P_2 that are neighboring each other in a Farey series associated with N and $Q_1/P_1 < Q_2/P_2$, namely,

$$P_1 Q_2 - P_2 Q_1 = 1. \tag{E2}$$

Inequality (4.11) can be derived directly from the above equation because $(1-E)^2 E^{P_1+P_2-1} <$[right-hand side of (E1)]$\leqslant E^{P_1+P_2-1} \leqslant E^N$, where the inequalities $0 \leqslant E < 1$ and $N < P_1 + P_2$ are taken into account.

We first note that the map $f(t)$ for region II can be derived by taking the limit $D \to \infty$ so that $r \to 0+$ in the map for region I. Then, taking the limit in Eqs. (C1) and (C2), we have the relations

$$S\left(\frac{Q}{P}\right) = S\left(\frac{Q_1}{P_1}\right) + E^{P_1} S\left(\frac{Q_2}{P_2}\right), \tag{E3}$$

$$T\left(\frac{Q}{P}\right) = T\left(\frac{Q_1}{P_1}\right) + E^{P_1} T\left(\frac{Q_2}{P_2}\right) \tag{E4}$$

for irreducible fractions satisfying (E2) and for the mediant $Q/P \equiv (Q_1+Q_2)/(P_1+P_2)$.

Using Eq. (E3), we can prove the following equation for any irreducible fraction Q/P, by induction:

$$S\left(\frac{Q}{P}\right) = \frac{1-E^P}{1-E}. \tag{E5}$$

Furthermore, using Eqs. (E3) and (E4), we can prove, by induction, the equation

$$S\left(\frac{Q_1}{P_1}\right) T\left(\frac{Q_2}{P_2}\right) - S\left(\frac{Q_2}{P_2}\right) T\left(\frac{Q_1}{P_1}\right) = E^{P_2-1}. \tag{E6}$$

Because

$$B_U\left(\frac{Q_2}{P_2}\right) - B_U\left(\frac{Q_1}{P_1}\right) = \frac{S\left(\frac{Q_1}{P_1}\right) T\left(\frac{Q_2}{P_2}\right) - S\left(\frac{Q_2}{P_2}\right) T\left(\frac{Q_1}{P_1}\right)}{S\left(\frac{Q_1}{P_1}\right) S\left(\frac{Q_2}{P_2}\right)} \tag{E7}$$

from Eq. (B1), Eqs. (E5) and (E6) lead to

$$B_U\left(\frac{Q_2}{P_2}\right) - B_U\left(\frac{Q_1}{P_1}\right) = \frac{(1-E)^2 E^{P_2-1}}{(1-E^{P_1})(1-E^{P_2})}. \tag{E8}$$

We can obtain $B_L(Q_2/P_2) - B_U(Q_1/P_1)$ using Eq. (E8) if we know $B_U(Q_2/P_2) - B_L(Q_2/P_2)$. For this purpose, we derive $B_L(Q_2/P_2)$ in the following. Let us consider a series of irreducible fractions

$$\frac{Q_1}{P_1}, \frac{Q_1+Q_2}{P_1+P_2}, \frac{Q_1+2Q_2}{P_1+2Q_2}, \ldots, \frac{Q_1+nQ_2}{P_1+nP_2}. \tag{E9}$$

Then, applying Eqs. (E3) and (E4) n times starting from the pair Q_1/P_1 and Q_2/P_2, we obtain

$$S\left(\frac{Q_1+nQ_2}{P_1+nP_2}\right) = S\left(\frac{Q_1}{P_1}\right) + S\left(\frac{Q_2}{P_2}\right) \sum_{k=0}^{n-1} E^{P_1+kP_2}, \tag{E10}$$

$$T\left(\frac{Q_1+nQ_2}{P_1+nP_2}\right) = T\left(\frac{Q_1}{P_1}\right) + T\left(\frac{Q_2}{P_2}\right) \sum_{k=0}^{n-1} E^{P_1+kP_2}. \tag{E11}$$

Substituting (E10) and (E11) into the expression for the lower boundary of $\mathcal{B}(Q_2/P_2)$,

$$\begin{aligned} B_L\left(\frac{Q_2}{P_2}\right) &= \lim_{n\to\infty} B_U\left(\frac{Q_1+nQ_2}{P_1+nP_2}\right) \\ &= \lim_{n\to\infty} T\left(\frac{Q_1+nQ_2}{P_1+nP_2}\right) \Big/ S\left(\frac{Q_1+nQ_2}{P_1+nP_2}\right), \end{aligned} \tag{E12}$$

we obtain

$$B_L\left(\frac{Q_2}{P_2}\right) = \frac{T\left(\frac{Q_1}{P_1}\right) + T\left(\frac{Q_2}{P_2}\right) G}{S\left(\frac{Q_1}{P_1}\right) + S\left(\frac{Q_2}{P_2}\right) G}, \tag{E13}$$

where

$$G = \frac{E^{P_1}}{1-E^{P_2}}. \tag{E14}$$

From Eqs. (B1), (E5), (E6), and (E13) we obtain

$$B_U\left(\frac{Q_2}{P_2}\right) - B_L\left(\frac{Q_2}{P_2}\right) = \frac{(1-E)^2 E^{P_2-1}}{1-E^{P_2}}. \tag{E15}$$

Using Eqs. (E8) and (E15), we obtain (E1).

[1] L. Glass and M. C. Mackey, J. Math. Biol. **7**, 339 (1979).
[2] G. A. Petrillo and L. Glass, Am. J. Phys. **246**, R311 (1984); M. Courtemanche, L. Glass, M. D. Rosengarten, and A. L. Goldberger, *ibid.* **257**, H693 (1989).
[3] L. Glass, CHAOS **1**, 13 (1991).
[4] E. Castigeras and R. Budelli, Physica D **56**, 235 (1992).
[5] K. Yagisawa, T. Kambara, and M. Naito, Phys. Rev. E **49**, 1320 (1994).
[6] D.-R. He, D. Wang, K.-J. Shi, C. Yang, L. Chao, and J. Zhang, Phys. Lett. A **136**, 363 (1989).
[7] B. Christiansen, D.-R. He, S. Habip, M. Bauer, U. Krueger, and W. Martienssen, Phys. Rev. A **45**, 8450 (1992).
[8] D.-R. He, B.-H. Wang, M. Bauer, S. Habip, U. Krueger, W. Martienssen, and B. Christiansen, Physica D **79**, 335 (1994).
[9] S. Habip, M. Bauer, D.-R. He, and W. Martienssen, Physica D **59**, 378 (1992).
[10] B. Christiansen, P. Alstrøm, and M. T. Levinsen, Phys. Rev. A **42**, 1891 (1990).
[11] J. P. Keener, Trans. Am. Math. Soc. **261**, 589 (1980).
[12] J. P. Keener, F. C. Hoppensteadt, and J. Rinzel, SIAM J. Appl. Math. **41**, 503 (1981).
[13] P. Alstrøm, Commun. Math. Phys. **104**, 581 (1986).
[14] P. Alstrøm, B. Christiansen, and M. T. Levinsen, Phys. Rev. Lett. **61**, 1679 (1988).
[15] M. Bauer, S. Habip, D.-R. He, and W. Martienssen, Phys. Rev. Lett. **68**, 1625 (1992).
[16] D.-R. He, M. Bauer, S. Habip, U. Krueger, W. Martienssen, B. Christiansen, and B.-H. Wang, Phys. Lett. A **171**, 61 (1992).
[17] F. Ji and D.-R. He, Phys. Lett. A **177**, 125 (1993).
[18] C. Wunderlich, L. Moorman, and P. M. Koch, Phys. Lett. A **176**, 317 (1993).
[19] R. Richter, A. Kittel, K. Pyragas, J. Peinke, and J. Parisi, Z. Phys. B **91**, 527 (1993).
[20] D.-R. He, E. J. Ding, M. Bauer, S. Habip, U. Krueger, W. Martienssen, and B. Christiansen, Europhys. Lett. **26**, 165 (1994).
[21] S.-X. Qu, B. Christiansen, and D.-R. He, Phys. Lett. A **201**, 413 (1995).
[22] S. Guan, B.-H. Wang, D.-K. Wang, and D.-R. He, Phys. Rev. E **52**, 453 (1995).
[23] P. Alstrøm, B. Christiansen, and M. T. Levinsen, Phys. Rev. B **41**, 1308 (1990).
[24] K. Yagisawa, M. Naito, K. Gondaira, and T. Kambara, Biophys. J. **64**, 1461 (1993).
[25] L. Glass and J. Bélair, in *Nonlinear Oscillations in Biology and Chemistry,* edited by H. G. Othmer, Lecture Notes in Biomathematics Vol. 66 (Springer-Verlag, Berlin, 1986), p. 232.
[26] K. Yagisawa, T. Kambara, N. Fuchikami, and M. Naito, Bull. Univ. Electro-Commun. (to be published).